The fate of ammonium in phengite at high temperature

Yan Yang, Vincent Busigny, Zhongping Wang, Qunke Xia

The fate of ammonium in phengite during high temperature processes

YAN YANG[1,*], VINCENT BUSIGNY[2], ZHONGPING WANG[3], QUNKE XIA[1]

[1] Institute of Geology and Geophysics, School of Earth Sciences, Zhejiang University, Hangzhou 310027, China

[2] Institut de Physique du Globe de Paris, Sorbonne Paris Cité, University Paris Diderot, UMR 7154 CNRS, F-75005 Paris, France

[3] Physics Experiment Teaching Center, University of Science and Technology of China, Hefei 230026, China

* Corresponding author

Institute of Geology and Geophysics

School of Earth Sciences

Zhejiang University

Hangzhou 310027, China

Email: yanyang2005@zju.edu.cn

ABSTRACT

Nitrogen (N) is the main component of the atmosphere and is largely considered as a volatile element. However, most researchers now agree that a significant amount of N, in the form of ammonium (NH_4^+) substituting for K^+ in some K-bearing minerals such as clays, micas, and feldspars, can be transferred to the deep Earth through subduction. The fate of ammonium in those minerals during subduction is still poorly known but is likely controlled by temperature and pressure pathways. In an attempt to contribute to understanding the fate of N during high temperature processes, we carried out *in situ* high temperature IR and Raman spectra measurements to investigate the rate and mechanism of NH_4^+ loss in phengite. We observed that a new OH band at 3425 cm^{-1} became prominent above 400 °C, and did not change with times during isothermal annealing at 500 and 700 °C. The N-H stretching band shifted to higher wavenumbers in the temperature interval from -150 to 20 °C, while linearly shifted to lower wavenumbers in the temperature interval from 20 to 500 °C and remained stable above 500 °C. The N-H bending band linearly shifted to lower wavenumbers in the temperature interval from -150 to 400 °C and remained stable. The K-O stretching

frequency decreased with increasing temperature to 600 °C, and then remained stable. These processes were reversible until dehydration and ammonium loss from phengite starting at 800 °C. The results suggest that (1) at low temperatures, ammonium is ordered and hydrogen bonding between ammonium and the framework evolves during cooling; (2) at high temperatures, the N-H interatomic distance of NH_4^+ lengthens with increasing temperature until 500 °C. N-H bond subsequently no longer lengthens, accompanied by H transferring from N to neighboring O and forming a new OH band at 3425 cm^{-1}. At 800 °C, H^+ starts breaking from N and leaving others to form NH_3 and OH^-. This study has implications for evaluating the extent to which these minerals can preserve information regarding nitrogen behavior during high temperature processes.

Keywords: phengite, nitrogen, ammonium, high temperature, IR, Raman

INTRODUCTION

Nitrogen (N) is an essential element for all living organisms. Although N is one of the predominant elements in the atmosphere and biosphere on Earth surface, it only accounts for 25–30% of the total planet inventory. Large amounts of N indeed reside in the deep Earth (Galloway 2003; Goldblatt et al. 2009; Palya et al. 2011; Busigny and Bebout 2013; Johnson and Goldblatt 2015). In sedimentary rocks, N occurs essentially as ammonium (NH_4^+) released from decomposed organic matter and is substituted for K^+ in some K-bearing minerals such as clays, micas, and feldspars (Williams et al. 1992). A significant amount of N, in the form of NH_4^+, can then be transferred to the deep Earth reservoir through subduction. The speciation of N in the Earth mantle is not very well constrained due to the very low N concentration and the poor degree of preservation of mantle rocks recovered at the surface (Yokochi et al. 2009). However, several recent theoretical and experimental studies suggested that NH_4^+ may be the main N species in most of the mantle (Watenphul et al. 2010; Li et al. 2013; Mikhail and Sverjensky 2014).

To address the N cycle in the deep Earth, extensive works have concerned the size and isotope composition of major crustal and upper-mantle N reservoirs (e.g., Cartigny

and Marty 2013 and references therein; Halama et al. 2014; Li et al. 2014). Recently, some studies reported N solubility in high-pressure minerals typical of deep Earth conditions (Li et al. 2013; Watenphul et al. 2009, 2010; Nobel 2016). Since subduction is the important mechanism for carrying N into deep reservoirs, it is crucial to determine the extent to which minerals can preserve NH_4^+ during deep subduction. Studies on sediments subducted to different depths show either a decrease or a preservation of N concentration with increasing metamorphic grade (Bebout and Fogel 1992; Mingram and Bräuer 2001; Busigny et al. 2003a; Plessen et al. 2010). One of the most important parameters for N stability or loss in subducting rocks was suggested to be the geothermal gradient, specifically temperature variations (Bebout et al. 1999a; Busigny et al. 2003a; Busigny and Bebout 2013). However, the diffusion rate and mechanism of NH_4^+ loss in the host minerals such as micas, alkali feldspar and clinopyroxene are still poorly known. Several studies have compared the rates of NH_4^+ loss and dehydration in some minerals, but there is still no consensus on rate and mechanism of NH_4^+ loss. For example, Higashi (1978, 2000) suggested that NH_4^+ loss was far ahead of dehydration in sericite (a fine grained variety of muscovite with chemical formula $K(AlFeMg)_2(SiAl)_4O_{10}(OH)_2.nH_2O$) based on differential thermal analysis. Other works argued that in NH_4-analcime, NH_4^+ loss and dehydration were parallel processes based on thermogravimetric and Fourier Transform Infrared (FTIR) spectrometry analyses (Miroshnichenko and Drebushchak 2003; Likhcheva et al. 2004). Using *in situ* high temperature FTIR spectra, Zhang et al. (2010) suggested that NH_4^+ loss in muscovite happened at temperatures near dehydration.

Phengite is the most common high-pressure white mica observed in subducted metasediments. Experimental works indicated that phengite was stable and could carry water to depths of about 300 km in subduction environment (Poli and Schmidt 1995; Domanik and Holloway 1996; Schmidt 1996; Schmidt and Poli 1998, 2014). Busigny et al. (2003b) reported that phengite from Western Italian Alps contained high NH_4^+ concentrations (up to 2000 ppm) in metasediments subducted down to ~90 km depth (3 GPa). Thus NH_4^+-bearing phengite represents an important component for N and H

transfer to the deep mantle (Watenphul et al. 2009; Bebout et al. 2016).

Since NH_4^+ substitutes for K^+ in the phengite structure, knowledge of evolutions of N-H bond and its host lattice at high temperature are necessary to understand the stability of NH_4^+ during the recycling process into the deep Earth. In the present study, we carried out *in situ* high temperature FTIR and Raman spectroscopic investigations of NH_4^+ and lattice framework in phengite respectively, and analyze their behavior at high temperature. We explored the temperature dependence of N-H and K-O length, and further figured out the rate and mechanism of NH_4^+ loss in phengite. The results have implications for better understanding the fate of ammonium in phengite during high-temperature processes.

MATERIALS AND METHODS

Sample description

Phengite crystals from a natural sample were used here as a starting material. They were extracted from a single high-pressure mestasediment of the western Alps (sample 98SE8). This sample was characterized in a previous study (Busigny et al., 2003b) and was selected for its high NH_4^+ content (~2000 ppm) in phengite, thus allowing relatively easy measurement by IR spectroscopy. The phengite powder was used for the X-ray diffraction measurement. Intensity data were collected using CuKα radiation with 2θ ranging from 3 to 70°. Based on the X-ray diffraction analysis (see supplementary material), this sample is trigonal. The unit-cell parameters of the sample are as following: a = 5.225 Å, b = 5.225 Å, c = 29.75 Å, α = β = 90°, γ = 120°. Figure 1 illustrates where ammonium is substituting into the phengite structure. The average chemical composition of the sample 98SE8 was reported in Busigny et al. (2003b): 55.6% SiO_2, 0.07% TiO_2, 21.03% Al_2O_3, 4.48% FeO, 0.05% MnO, 4.42% MgO, 0.00% CaO, 0.04% Na_2O. The size of the crystals ranged between 0.2 and 2 mm. The thickness of the analyzed grains ranged from 0.01 to 0.12 mm.

Low and high temperature FTIR spectroscopy

For the *in situ* low temperature measurement, the phengite sample was placed on

an Al foil with a hole of 1.5 mm in diameter in a Linkam FTIR600 heating/cooling stage with ZnSe windows. The temperature step was regulated by a Linkam TMS94 controller with 0.1 ˚C accuracy. The sample was cooled successively from room temperature to 0 ˚C, -50 ˚C, -100 ˚C and -150 ˚C at a cooling rate of 10 ˚C/min. For every temperature step, the dwell time was 10 minutes.

For the *in situ* high temperature measurement, the phengite sample was placed on a Pt foil with a hole of 1.5 mm in diameter in an Instec HS1300 heating stage with CaF_2 windows, equipped with a resistance heater and an S type thermocouple. The sample was heated in Ar and air, respectively. The sample temperature was determined with a typical uncertainty of less than 1 °C. The temperature was initially increased from 20 to 100 ˚C, and then by 100 ˚C increments to 800 ˚C, using a heating rate of 15 ˚C/min. For every temperature step, the dwell time was 5 minutes. The *In situ* FTIR measurements in isothermal annealing were conducted using the procedure described by Okumura and Nakashima (2006): the temperature of the heating stage was elevated at a rate of 100 °C /min and held at a desired temperature. After collecting the background FTIR spectrum at the desired temperature, a phengite grain was put in the heating stage and the initial sample FTIR spectrum was measured just after the sample was set.

To compare rate of dehydration and ammonium loss, FTIR measurements on quenched samples were conducted. Two thin phengite grains (about 0.01 and 0.03 mm thickness) were heated in the heating stage purged with Ar at a desired temperature of 750 and 800 ˚C for 30 minutes, respectively. Then FTIR measurements were carried out on the samples quenched to room temperature.

FTIR spectra in the frequency range 4000-1000 cm^{-1} were collected with an IR beam direction perpendicular to the (001) plane (i.e. to the layer) using a Nicolet iS50 FTIR spectrometer coupled with a Continuμm microscope. A KBr beam-splitter and a liquid nitrogen-cooled MCT-A detector were used. A total of 128 scans were accumulated for each spectrum at a 4 cm^{-1} resolution. The aperture size was set to 50×50 μm. Spectra were collected on the same selected area for every sample.

In situ high temperature Raman spectroscopy

The phengite sample was placed on a Pt foil in a Linkam TS1500 heating stage, equipped with a resistance heater and an S type thermocouple. The sample temperature was determined with a typical uncertainty of less than 1 °C. The automatic temperature control unit was programmed to set the heating rate at 20 ˚C/min to reach the desired temperature. The dwelling time amounted to 5 minutes at each experimental temperature.

In situ high temperature Raman spectroscopic analyses were performed with the incident laser beam perpendicular to the (001) plane on a LABRAM-HR spectrometer with 1800 g/mm gratings. Single-crystal silicon was used as a reference. Raman spectra in the frequency range 50-1200 cm^{-1} were collected at room temperature and from 100 to 800 °C at 100 °C interval. The focal length for the spectrograph was 750 mm. The sample was excited by the 514.5 nm green light of a Spectra Physics Ar ion laser. A 50X objective was used to focus the incident laser light on the sample and to collect the scattered light. The diameter of the focused laser light spot was estimated to be 10 μm.

Data analysis

OriginPro 8.0 software was used to analyze IR and Raman spectra at various temperatures.

RESULTS

FTIR spectra of NH_4^+ in phengite at room temperature

There are four normal vibrational modes in isolated ammonium: symmetric (ν_1), and antisymmetric (ν_3) stretching vibrations, as well as symmetric (ν_2) and antisymmetric (ν_4) bending vibrations (Herzberg 1966; Kearley and Oxton 1983). Of these, only ν_3 and ν_4 are IR active. However, for ammonium in a crystal, ν_1 and ν_2 bands may appear in IR spectra due to decreased symmetry. FTIR spectroscopy is very sensitive to N-H vibrations and has been used to analyze NH_4^+ in minerals in previous studies (e.g., Busigny et al. 2003b; Watenphul et al., 2009, 2010; Zhang et al. 2010;

Wunder et al. 2015; Vennari et al. 2016). The polarized and unpolarized IR spectra of NH_4^+ in phengite at room temperature are shown in Figure 2. Following the band assignments from Harlov et al. (2001), Busigny et al. (2003b) and Watenphul et al. (2009) (Table 1), the band at 3291 cm^{-1} corresponds to ν_3-asymmetric stretching mode while the one at 3036 cm^{-1} reflects a combination of ν_2-symmetric and ν_4-antisymmetric bending vibrations. The band at 1430 cm^{-1} corresponds to ν_4 and its corresponding overtone $2\nu_4$ is at 2818 cm^{-1}. Since using an IR beam perpendicular to the (001) plane represents isotropic properties independent from orientation, there is little difference in the absorption of NH_4^+ or OH with the polarizer rotating different angles as shown in Figure 2. Therefore, in the present contribution, we used unpolarized radiation to study ammonium in phengite under different temperatures, as was also applied by Zhang et al. (2010) to study OH and ammonium in muscovite.

In situ FTIR spectra of NH_4^+ in phengite at different temperatures

Upon cooling, the bands are intensive, sharp and peak splitting. We can clearly distinguish four new bands at 3219, 3117, 2880 and 1404 cm^{-1} as the temperature is decreased down to -150 °C (Fig. 3). Those bands are assigned to the vibrations of ammonium (Reed and Williams 2006; Watenphul et al. 2009; Wunder et al. 2015). At high temperatures, changes of the IR spectra with increasing temperature under air and Ar atmospheres are similar, with all bands becoming significantly broad and overlapping (Fig. 4). Most interestingly, a new band at 3425 cm^{-1} becomes prominent above 400 °C. The appearance of this new band is unquenchable, and does not exist in the spectrum at room temperature after heating. The combination of NH_4^+ symmetric and antisymmetric bending band ($\nu_2 + \nu_4$) at 3036 cm^{-1} and the overtone antisymmetric bending band ($2\nu_4$) at 2818 cm^{-1} disappear at 200 °C, while the N-H stretching band (ν_3) at 3291 cm^{-1} and bending band (ν_4) at 1430 cm^{-1} still remain up to 800 °C. The evolution of frequencies of the bands of ν_3 and ν_4 with temperature is plotted in Figure 5. With increasing temperature, the ν_3 band shifts to higher wavenumbers from -150 to 20 °C, while linearly shifts to lower wavenumbers from 20 to 500 °C and remains stable above 500 °C. The ν_4 band linearly shifts to lower wavenumbers with increasing

temperature from -150 to 400 °C and remains stable.

In situ FTIR spectra of NH_4^+ in isothermal annealing and on quenched samples

To investigate the stability of NH_4^+, we carried out *in situ* FTIR measurements in isothermal annealing at 500 and 700 °C in air, respectively. Figure 6 displays *in situ* IR spectra collected at different time intervals. At the two different temperatures explored herein, the IR absorptions of the new band at 3425 cm^{-1} and ammonium bands do not change with heating times. In addition, the IR spectra are the same at room temperature before and after heating. It should be noted that the weakening of the absorptions at high temperatures compared to room temperature is mainly induced by decreasing absorption coefficient with increasing temperature (e.g., Zhang et al. 2007; Tokiwai and Nakashima 2010; Yang et al. 2010, 2012; Radica et al. 2016).

We cannot investigate the stability of water in phengite from data presented in Figure 6 since the detector of IR spectrometer is oversaturated for measuring absorption of OH band around 3610 cm^{-1} using the thick sample. To overcome this problem and compare the starting temperature of dehydration and loss of ammonium, we use much thinner samples (<30 μm). We collected IR spectra of the thinner phengite flakes quenched from 750 and 800 °C, respectively (Fig. 7). The absorptions of both OH and NH_4^+ at room temperature before and after heating to 750 °C for 30 minutes are almost the same, indicating that water and ammonium in phengite still can be preserved to 750 °C. In contrast, the absorptions of OH and NH_4^+ distinctly decrease comparing the spectra at room temperature before and after heating to 800 °C for 30 minutes. The integrated absorptions of NH_4^+ from 2800 to 3400 cm^{-1} and 1340 to 1500 cm^{-1} are reduced by 45.8% and 73.1%, respectively, and the integrated absorptions of OH around 3610 cm^{-1} decrease by 25.8%. As a result, dehydration and loss of ammonium in phengite start at the same temperature around 800 °C, which supports previous arguments that ammonium loss and dehydration were parallel processes in analcime and muscovite (Miroshnichenko and Drebushchak 2003; Likhcheva et al. 2004; Zhang et al. 2010).

In situ Raman spectra of lattice vibrations in phengite at high temperatures

Raman spectroscopy is sensitive to local structural environment within crystal and usually used to study lattice vibrations. The Raman spectra of phengite at different temperatures are displayed in the range 50-1200 cm^{-1} (Fig. 8). There are four most prominent bands at 104, 192, 270, and 706 cm^{-1} in the spectrum at room temperature (25 °C). The band assignments are listed in Table 1. Based on lattice dynamic calculations, McKeown et al. (1999) suggested that modes between 800 and 360 cm^{-1} had internal tetrahedral sheet motions mixed with K and octahedral Al displacements, and modes at frequencies less than 360 cm^{-1} had lattice motions. In the present study, the band at 104 cm^{-1} is due to K-O stretching vibration according to band assignment of Holtz et al. (1993), McKeown et al. (1999), Mookherjee and Redfern (2002), Zhang et al. (2010) and Williams et al. (2012). Figure 9 displays the mode frequency shifts with temperature. The bands at 192, 270 and 706 cm^{-1} linearly shift to lower Raman frequencies, indicating expansion of the microstructure with increasing temperature. Among these bands, the K-O stretching band at 104 cm^{-1} exhibits interesting temperature dependence. The band frequency decreases with increasing temperature to 600 °C, then remains stable.

DISCUSSION

The local environment of the ammonium in phengite at low temperature

Pauling (1930) expressed orientational ordering of a tetrahedral molecule such as ammonium and suggested the possibility of a transition from free rotation or tumbling of the ammonium to oscillatory motion on cooling. At room temperature, ammonium freely tumbles and the site symmetry is essentially spherical. Upon cooling, the ammonium freezes into one orientation, multiple equivalent orientations, or hindered oscillation, changing the symmetry with a loss of degeneracy, peak splitting, as well as line narrowing. Mookherjee et al. (2002a and 2002b) observed the peak splitting of ammonium in the IR spectra of tobelite and phlogopite at low temperatures and attributed it to a disorder/order transition of the ammonium. Similarly, the splitting and

narrowing IR bands of ammonium during cooling in this study indicates the ordering of ammonium in phengite at low temperatures. Thus a discrete hydrogen bonding between ammonium and the framework evolves at low temperatures. The presence of hydrogen bonding at low temperatures can also be indicated from the lower frequency shift of ν_3 and higher frequency shift of ν_4 (Plumb and Hornig 1955). Figure 5 shows that the frequencies of ν_3 and ν_4 change from 3291 and 1430 cm^{-1} at room temperature to 3286 and 1433 cm^{-1} at -150 ^{o}C, respectively, suggesting the presence of hydrogen bonding at low temperatures.

Origin of the new band at 3425 cm^{-1}

The source of this new band at 3425 cm^{-1} may has two possibilities. First, the NH_3 molecule has four normal modes at 3336 (ν_1), 950 (ν_2), 3444 (ν_3) and 1626 cm^{-1} (ν_4) in the gaseous state (Buback and Schulz 1976). Thus, it may result from the 3444 (ν_3) mode of NH_3. Second, it is due to O-H vibration. In this study, we exclude the first possibility and ascribe it to the O-H vibration based on the following reasons. (1) Ammonium in phengite does not dissociate until 800 °C. Thus the appearance of the new band at 400 °C is not likely related to NH_3 gas. (2) The IR spectra in this study were recorded from samples heating in open system in air or flushed with Ar. The absorption of the new band does not vary with time during *in situ* isothermal annealing and is not quenchable, which is unlikely for NH_3 gas being very mobile. The new OH band is very weak compared to the original OH band in phengite, indicating it is not the inherent water. Zhang et al. (2010) also observed a new band around 3428 cm^{-1} at 327-427 °C from the *in situ* high temperature IR spectra of muscovite. They ascribed it to OH resulting from protons migrating to new locations or change of OH environments at the atomic level with increasing temperature.

Evolutions of K-O and ammonium vibrations with temperature

Ammonium locates in the interlayer substituting for K in the phengite (Vedder 1965). Thus acknowledgement of high temperature behavior of interlayer is necessary to understand evolutions of ammonium at high temperatures. Considering the relatively

low content of ammonium in the sample, the high temperature behavior of the interlayer is likely primarily controlled by K. The Raman spectroscopic study shows the decrease of vibration frequency at 104 cm^{-1} corresponding to K-O vibration with increasing temperature to 600 °C. Based on bond length, K-O bond can be divided into $K\text{-}O_{inner}$ which is shorter and $K\text{-}O_{outer}$ which is longer (Tateyama *et al*. 1977). The band at 104 cm^{-1} was attributed to stretching vibration of $K\text{-}O_{inner}$ (Mookherjee and Redfern 2002; Zhang et al. 2010). Thus the decrease of vibration frequency at 104 cm^{-1} with increasing temperature indicates the lengthening of $K\text{-}O_{inner}$ bond, consistent with the increase in length of the $K\text{-}O_{inner}$ bonds with increasing temperature as observed by neutron diffraction and X-ray diffraction (Guggenheim et al. 1987; Mookherjee et al. 2011; Gemmi et al. 2008). The K-O vibration does not change after 600 °C, indicating K-O bond no longer lengthens. Guggenheim et al. (1987) proposed that dehydroxylation in muscovite started with lengthening of K-O2 relative to the other two interlayer bonds, thus this discontinuity in lengthening of K-O bond may be precursory to thermal decomposition or dehydroxylation of the phengite.

The broad and overlapping bands of ammonium at high temperatures suggest ordering of ammonium does not occur during heating. In addition, because of thermal expansion of the interlayer sites and lengthening of K-O bonds, hydrogen bonding between ammonium and silicate framework at high temperatures would be negligible. However, hydrogen bonding can appear under low temperatures such as -150 °C stated above because the interlayer distance decreases leading to an increased interaction between ammonium and silicate framework.

Previous studies suggested that positive frequency shift with increasing pressure typically indicate an increase in bond strength generated by compression, while negative frequency shift with increasing pressure in hydrogen stretching vibrations are associated with increases in hydrogen bonding (and hence weakening of the primary anion-H bond) (e.g., Cynn and Hofmeister 1994; Vennari et al. 2016). In contrast to pressure-induced frequency shift, negative shift of frequency with increasing temperature in vibration spectra typically indicates a weakening in bond strength

316 generated by expansion, while positive shift of frequency of hydrogen stretching
317 vibrations with increasing temperature is associated with weakening hydrogen bonding
318 (and hence strengthening of the primary anion-H bond) (Aines and Rossman 1985; Xu
319 et al. 2013; Yang et al. 2015; Thompson et al. 2016). Thus, under low temperatures, the
320 positive frequency shift of N-H stretching band with increasing temperature may
321 indicate hydrogen bonding is the dominant effect. With increasing temperature,
322 hydrogen bond weakens, thereby N-H strengthens. With increasing temperatures above
323 20 °C, hydrogen bond is too weak to be the dominant effect. Therefore, at high
324 temperatures, the negative frequency shift of N-H stretching vibration with increasing
325 temperature from 20 to 500 °C indicates that lengthening of N-H bond rather than
326 hydrogen bonding is the dominant effect. On further heating above 500 °C, the N-H
327 stretching frequency remains stable, suggesting that the N-H bond no longer lengthens.
328 The bending vibration of ammonium exhibits the similar high temperature behavior
329 with a discontinuity at 400 °C. This probably accounts for the occurrence of the new
330 OH band at 3425 cm^{-1} during heating, with H transferring from N to the adjacent O and
331 forming O-H. The proton transferring process is reversible with H transferring from O
332 back to N after being quenched.

333 **Mechanism of ammonium loss in phengite**

334 In our experiment, loss of ammonium in phengite starts at 800 °C and is
335 synchronized with dehydration. The results of the present study are consistent with
336 Zhang et al. (2010) and support their conclusion that ammonium loss in muscovite took
337 place at temperatures near dehydration. Based on the above discussion about evolutions
338 of K-O and ammonium bonds with temperatures and origin of the new OH band, we
339 propose the processes involved in ammonium loss illustrated in Figure 10. With
340 increasing temperature, the N-H interatomic distance of NH_4^+ lengthens until 500 °C.
341 N-H bond subsequently no longer lengthens, accompanied by H transferring from N to
342 neighboring O (likely a basal oxygen in the Si_6O_8 ring) and forming a new OH band at
343 3425 cm^{-1}. The process is reversible and ammonium does not dissociate until the
344 temperature is increased to 800 °C. At 800 °C, H^+ starts breaking from N, leaving others

forming NH_3 and OH^-, just similar to the decomposition of NH_4-analcime ($NH_4^+ + O_2^- = NH_3 + OH^-$) and NH_4Cl ($NH_4^+ + Cl^- = NH_3 + HCl$) (Likhacheva et al. 2004; Schmidt and Watenphul 2010). Unfortunately, we did not observe the band of NH_3 vibrations in the IR spectra at high temperatures because of the trace amounts of ammonium in phengite and the open system. However, Likhacheva et al. (2004) indeed found the band around 1626 cm^{-1} of NH_3 in high temperature IR spectra of NH_4-analcime. Schmidt and Watenphul (2010) also observed the formation of NH_3 at high temperatures based on the appearance of the band around 3310 cm^{-1} in the high temperature Raman spectra of NH_4Cl. Conclusively, the results of our study suggest that the first step of NH_4^+ loss in phengite corresponds to the following reaction: $NH_4^+ + O^{2-} = NH_3 + OH^-$, which is consistent with the mechanism proposed for degassing of NH_4-analcime (Likhacheva et al. 2004).

Concerning the products of thermal decomposition of NH_4^+ in minerals, some studies reported NH_3 (e.g., Weeks et al. 1975; Beyer et al. 1977; Likhacheva et al. 2004), while other experiments obtained no NH_3 but N_2 in the products (e.g., Whelan et al. 1988). Haendel et al. (1986) suggested a second process of further conversion of NH_3 to N_2 at elevated temperatures and thus explained the controversy. For the thermal decomposition of NH_3 to N_2, it follows the slightly endothermic reaction (Cheddie 2012): $2NH_3 + 94.2\ KJ = N_2 + 3H_2$. Thus NH_3 is not stable at high temperatures and begins to decompose at 200 °C (Lan et al. 2012) from thermodynamic analysis. However, the reaction rate depends on temperature as well as catalysts. According to the rate of reaction with catalyst at 800 °C (Li et al. 2009), the fraction of remaining NH_3 was up to 90% after heating for one hour. In this study, no catalyst was introduced during the heating process and the dwelling time was at most 30 minutes at 800 °C. As a result, under the conditions of the present study, the second step is not involved and the product of NH_4^+ decomposition in phengite is most likely dominated by NH_3. Previous spectroscopic study on NH_4^+ in fluid (NH_4Cl) also showed that a significant amount of NH_4^+ was converted to NH_3 at high temperatures (Schmidt and Watenphul 2010).

Although NH_3 is the product of the first step of NH_4^+ decomposition in minerals, the second step involving NH_3 decomposition to N_2 hence could potentially be efficient in natural environment and at geological time scales, because of the existing abundance of catalysts (e.g., Fe_2O_3, CuO, CaO, ZnO, MnO_2, TiO_2, SiO_2, V_2O_5, etc.) in geological conditions. This is witnessed for instance by the observation that several high temperature metamorphic rocks are compatible with a release of N_2 rather than NH_3 (e.g., Duit et al. 1986; Bebout and Fogel 1992; Svensen et al. 2008). These effects of catalysts and temperature should be tested further in future experimental studies, specifically exploring variable parameters affecting NH_4^+ fate in high temperature systems.

IMPLICATIONS

From the results obtained herein by IR and Raman spectroscopic analysis of phengite at different temperatures, the following conclusions can be drawn. (1) Dehydration and loss of ammonium in phengite start at the same temperature of 800 °C. (2) The mechanism of NH_4^+ loss involves the following process: during heating, the N-H interatomic distance of NH_4^+ lengthens until 500 °C and subsequently no longer lengthens accompanied by H transferring from N to O and forming a new OH band at 3425 cm^{-1}. The process is reversible and ammonium does not dissociate until 800 °C. At 800 °C, H^+ starts breaking from N, leaving others forming NH_3 following the reaction: $NH_4^+ + O^{2-} = NH_3 + OH^-$.

The results of this study imply that phengite cannot preserve a large amount of NH_4^+ in its structure under high temperature conditions (i.e. > 700 °C) even in Ar atmosphere. This finding is in good agreement with general observation that samples subducted along high geothermal gradients experienced drastic N devolatilization with increasing metamorphic conditions, while samples from cooler subduction zones retained N (Bebout and Fogel 1992; Mingram and Bräuer 2001; Busigny et al. 2003a; Elkins et al. 2006; Mitchell et al. 2010; Plessen et al. 2010). The strong temperature dependence of N content during metamorphism was also illustrated by previous work in continental geological settings. For instance, studies on mica-bearing metasediments

heated by granitic intrusion demonstrated that bulk-rock N content decreased along a profile toward the granite contact (e.g., Bebout et al. 1999b; Jia 2006). Nitrogen was released at temperature higher than ~500 °C, which is slightly lower than the temperature identified in the present laboratory experiment. The distinct temperatures of N devolatilization may reflect that (1) natural metasediments are not made of a single N-bearing mineral (i.e. phengite in the present experiment) but correspond to complex matrixes including muscovite, biotite, and K-feldspars, or that (2) a kinetic effect controls partly NH_4^+ destabilization in micas since metasediments were left at high temperature over geological timescale (several Ma), which contrasts with the 30 minutes of the present experiment. Longer laboratory experiments should be designed to test this possibility. Finally, to further address the N cycle in deep Earth, kinetics of NH_4^+ loss in phengite and other NH_4^+-bearing minerals in the mantle (e.g., clinopyroxene) need to be investigated in future work.

ACKNOWLEDGMENTS

This work was supported by the Fundamental Research Funds for the Central Universities (2016QNA3014). Vincent Busigny was funded by the Research Program SYSTER-2012 of the Institut National des Sciences de l'Univers. Comments and suggestions from two anonymous reviewers helped to improve the manuscript. The authors also warmly thank Warren Huff for editing the manuscript.

REFERENCES

Aines, R.D. and Rossman, G.R. (1985) The high temperature behavior of trace hydrous components in silicate minerals. American Mineralogist, 70: 1169-1179.

Bebout, G.E. and Fogel, M. (1992) Nitrogen-isotope compositions of metasedimentary rocks in the Catalina Schist, California: Implications for metamorphic devolatilization history. Geochimica et Cosmochimica Acta, 56: 2839-2849.

Bebout, G.E., Ryan, J.G., Leeman, W.P, and Bebout, A.E. (1999a) Fractionation of trace elements by subduction-zone metamorphism-effect of convergent-margin thermal

430 evolution. Earth and Planetary Science Letters, 171: 63-81.

431 Bebout G.E., Cooper D.C., Don Bradley A., and Sadofsky S.J. (1999b) Nitrogen-
432 isotope record of fluid-rock interactions in the Skiddaw Aureole and granite,
433 English Lake District. American Mineralogist, 84: 1495-1505.

434 Bebout, G.E., Lazzeri, K.E., and Geiger, C.A. (2016) Pathways for nitrogen cycling in
435 Earth's crust and upper mantle: A review and new results for microporous beryl
436 and cordierite. Ammerican Mineralogist, 101: 7-24.

437 Beyer, H.K., Jacobs, P.A., Uytterhoeven, J.B., and Till, F. (1977) Thermal stability of
438 NH_4-chabazite. Journal of the Chemical Society Faraday Transactions, 73: 1111-
439 1118.

440 Buback, M. and Schulz, K.R. (1976) Raman Scattering of Pure Ammonia to High
441 Pressures and Temperatures. Journal of Physics and Chemistry, 80: 2478-2482.

442 Busigny, V., Cartigny, P., Philippot, P., Ader, M., and Javoy, M. (2003a) Massive
443 recycling of nitrogen and other fluid-mobile elements (K, Rb, Cs, H) in a cold slab
444 environment: evidence from HP to UHP oceanic metasediments of the Schistes
445 Lustrés nappe (western Alps, Europe). Earth and Planetary Science Letters, 215:
446 27-42.

447 Busigny, V., Cartigny, P., Philippot, P., and Javoy, M. (2003b) Ammonium
448 quantification in muscovite by infrared spectroscopy. Chemical Geology, 198: 21-
449 31.

450 Busigny, V. and Bebout, G.E. (2013) Nitrogen in the silicate Earth: Speciation and
451 isotopic behavior during mineral-fluid interactions. Elements, 9: 353-358.

452 Cartigny, P. and Marty, B. (2013) Nitrogen isotopes and mantle geodynamics: The
453 emergence of life and the atmosphere-crust-mantle connection. Elements, 9: 359-
454 366.

455 Cheddie, D. (2012) Ammonia as a hydrogen source for fuel cells: a review. In: Minic,
456 D., Ed., Hydrogen Energy-Challenges and Perspectives, Intech, Rijeka, 333-362.

457 Cynn, H. and Hofmeister, A.M. (1994) High-pressure IR spectra of lattice modes and
458 OH vibrations in Fe-bearing wadsleyite. Journal of Geophysical Research, 99:
459 17717-17727.

460 Domanik, K.J. and Holloway, J.R. (1996) The stability and composition of phengitic
461 muscovite and associated phases from 5.5 to 11 GPa: Implications for deeply
462 subducted sendiments. Geochimica et Cosmochimica Acta, 60: 4133-4150.

463 Duit, W., Jansen, J.B.H., van Breeman, A., and Bos, A. (1986) Ammonium micas in
464 metamorphic rocks as exemplified by Dome de L'Agout (France). American
465 Journal of Science, 286: 702-732.

466 Elkins, L., Fischer, T., Hilton, D., Sharp, Z., McKnight, S., and Walker, J. (2006)
467 Tracing nitrogen in volcanic and geothermal volatiles from the Nicaraguan
468 volcanic front. Geochimica et Cosmochimica Acta, 70: 5125-5235.

469 Galloway, J.N. (2003) The global nitrogen cycle. In Treatise on Geochemistry, chapter
470 8.12, p. 557-583. Elsevier, Amsterdam.

471 Gemmi, M., Merlini, M., Pavese, A., and Curetti, N. (2008) Thermal expansion and
472 dehydroxylation of phengite micas. Physics and Chemistry of Minerals, 35: 367-
473 379.

474 Guggenheim, S., Chang, Yu-H., and Koster van Groos, A.F. (1987) Muscovite
475 dehydroxylation: High-temperature studies. American Mineralogist, 72: 537-550.

476 Goldblatt, C., Claire, M.W., Lenton, T.M., Matthews, A.J., Watson, A.J., and Zahnle,
477 K.J. (2009) Nitrogen enhanced greenhouse warming on early Earth. Nature
478 Geoscience, 2: 891-896.

479 Halama, R., Bebout, G.E., John, T., and Scambelluri, M. (2014) Nitrogen recycling in
480 subducted mantle rocks and implications for the global nitrogen cycle.
481 International Journal of Earth Sciences (Geol Rundsch), 103: 2081-2099.

482 Haendel, D., Muhle, K., Nitzsche, H.M., Stiehl, G., and Wand, U. (1986) Isotopic
483 variations of the fixed nitrogen in metamorphic rocks. Geochimica et

484 Cosmochimica Acta, 50: 749-758.

485 Harlov, D.E., Andrut, M., and Pöter, B. (2001) Characterization of buddingtonite (NH_4)
486 ($AlSi_3O_8$) and ND_4-buddingtonite (ND_4)($AlSi_3O_8$) using IR spectroscopy and
487 Rietveld refinement of XRD spectra. Physics and Chemistry of Minerals, 28: 188-
488 198.

489 Herzberg, G. (1966) Molecular spectra and molecular structure Vol.2: Infrared and
490 Raman spectra of polyatomic molecules. Van Nostrand, Princton.

491 Higashi, S. (1978) Dioctahedral mica minerals with ammonium ions. Journal of
492 Mineralogical and Petrological, 9: 16-27.

493 Higashi, S. (2000) Ammonium-bearing mica and mica/smectite of several pottery stone
494 and pyrophyllite deposits in Japan: Their mineralogical properties and utilization.
495 Applied Clay Science, 16: 171-184.

496 Holtz, M., Solin, S.A., and Pinnavaia, T.J. (1993) Effect of pressure on the Raman
497 vibrational modes of layered aluminosilicate compounds. Physical Review B,
498 13313-13317.

499 Ivaldi, G., Ferraris, G., Guretti, N., and Compagnoni, R. (2001) Coexisting 3T and
500 2M_1 polytypes of phengite from Cima Pal (Val Savenca, western Alps):
501 Chemical and polytypic zoning and structural characterization. European Journal
502 of Mineralogy, 13: 1025-1034.

503 Jia Y. (2006) Nitrogen isotope fractionations during progressive metamorphism: A case
504 study from the Paleozoic Cooma metasedimentary complex, southeastern
505 Australia. Geochimica et Cosmochimica Acta, 70: 5201-5214.

506 Johnson, B. and Goldblatt, C. (2015) The nitrogen budge of Earth. Earth-Science
507 Reviews, 148: 150-173.

508 Kearley, G.J. and Oxton, L.A. (1983) Recent advances in the vibrational spectroscopy
509 of ammonium ion in crystal. In R.J.H. Clark and R.E. Hesters, Eds., Advances in
510 Infrared and Raman Spectroscopy, 10, Chapter 2. John Wiley and Sons, New York.

511 Lan, R., Irvine, J.T.S., and Tao, S. (2012) Ammonia and related chemicals as potential
512 indirect hydrogen storage materials. International Journal of Hydrogen Energy, 37:
513 1482-1494.

514 Li, L., Cartigny, P., and Ader, M. (2009) Kinetic nitrogen isotope fractionation
515 associated with thermal decomposition of NH_3: Experimental results and potential
516 applications to trace the origin of N_2 in natural gas and hydrothermal systems.
517 Geochimica et Cosmochimica Acta, 73: 6282-6297.

518 Li, L., Zheng, Y.F., Cartigny, P., and Li, J. (2014) Anomalous nitrogen isotopes in
519 ultrahigh-pressure metamorphic rocks from the Sulu orogenic belt: Effect of
520 abiotic nitrogen reduction during fluid-rock interaction. Earth and Planetary
521 Science Letters, 403: 67-78.

522 Li, Y., Wiedenbeck, M., Shcheka, S., and Keppler, H. (2013) Nitrogen solubility in
523 upper mantle minerals. Earth and Planetary Science Letters, 377: 311-323.

524 Likhacheva, A.Y., Veniaminov, S.A., and Paukshtis, E.A. (2004) Thermal
525 decomposition of NH_4-analcime. Physics and Chemistry of Minerals, 31: 306-312.

526 McKeown, D.A., Bell, M.L., and Etz, E. (1999) Vibrational analysis of the dioctahedral
527 mica: 2M1 muscovite. American Mineralogist, 84: 1041-1048.

528 Mikhail, S. and Sverjensky, D.A. (2014) Nitrogen speciation in upper mantle fluids and
529 the origin of Earth's nitrogen-rich atmosphere. Nature Geoscience, 7: 816-819.

530 Mingram, B. and Bräuer, K. (2001) Ammonium concentration and nitrogen isotope
531 composition in metasedimentary rocks from different tectonometamorphic units
532 of the European Variscan Belt. Geochimica et Cosmochimica Acta, 65: 273-287.

533 Miroshnichenko, Y.M. and Drebushchak, V.A. (2003) Thermal decomposition of NH_4-
534 analcime: A kinetic study. Geophysical Research Abstract, vol. 5, 00298
535 (European Geophysical Society 2003).

536 Mitchell, E.C., Fischer, T.P., Hilton, D.R., Hauri, E.H., Shaw, A.M., de Moor, J.M.,
537 Sharp, Z.D., and Kazahaya, K. (2010) Nitrogen souces and recycling at subduction

538 zones: Insights from the bizu-Bonin-Mariana arc. Geochemistry Geophysics
539 Geosystems, 11: 1448-1470.

540 Mookherjee, M., Redfern, S.A.T., and Zhang, M. (2001) Thermal response of structure
541 and hydroxyl ion of phengite 2M1: an in situ neutron diffraction and FTIR study.
542 European Journal of Mineralogy, 13: 545-555.

543 Mookherjee, M. and Redfern, S.A.T. (2002) A high-temperature Fourier transform
544 infrared study of the interlayer and Si-O-stretching region in phengite-$2M_1$. Clay
545 Minerals, 37: 323-336.

546 Mookherjee, M., Redfern, S.A.T., Zhang, M., and Harlov, D.E. (2002a) Orientational
547 order-disorder in synthetic ND_4/NH_4-phlogopite: a low-temperature infrared study.
548 European Journal of Mineralogy, 14: 1033-1039.

549 Mookherjee, M., Redfern, S.A.T., Zhang, M., Harlov, and D.E. (2002b) Orientational
550 order-disorder of $N(D,H)_4^+$ in tobelite. American Mineralogist, 87: 1686-1691.

551 Nobel, S.M. (2016) Solubility of nitrogen in stishovite: A possible storage mechanism
552 for nitrogen in Earth's deep interior: [D]. Arizona State University.

553 Okumura, S. and Nakashima, S. (2005) Molar absorptivities of OH and H2O in rhyolitic
554 glass at room temperature and at 400-600 ℃. American Mineralogist, 90: 441-447.

555 Palya, A.P., Buick, I.S., and Bebout, G.E. (2011) Storage and mobility of nitrogen in
556 the continental crust: Evidence from partially melted metasedimentary rocks, Mt.
557 Stafford, Australia. Chemical Geology, 281: 211-226.

558 Pauling, L. (1930) Rotational motion of molecules in crystals. Physics Review, 36: 430-
559 443.

560 Plessen, B., Harlov, D.E., Henry, D., and Guidotti C.V. (2010) Ammonium loss and
561 nitrogen isotopic fractionation in biotite as a function of metamorphic grade in
562 metapelites from western Maine, USA. Geochimica et Cosmochimica Acta, 74:
563 4759-4771.

564 Plumb, R.C. and Hornig, D.F. (1950) Infrared spectrum, X-ray diffraction pattern, and
565 structure of ammonium fluoride. The Journal of Physical Chemistry, 23: 947-953.

566 Poli, S. and Schmidt, M.W. (1995) H_2O transport and release in subduction zones-
567 experimental constraints on basaltic and andesitic systems. Journal of Geophysical
568 Research, 100: 22299-314.

569 Reed, J.W. and Williams, Q. (2006) An infrared spectroscopic study of NH_4Br-
570 ammonium bromide to 55 GPa. Solid State Communications, 140: 202-207.

571 Schmidt, C. and Watenphul, A. (2010) Ammonium in aqueous fluids to 600℃, 1.3 GPa:
572 A spectroscopic study on the effects on fluid properties, silica solubility, and K-
573 feldspar to muscovite reactions. Geochimica et Cosmochimica Acta, 74: 6852-
574 6866.

575 Schmidt, M.W. (1996) Experimental constraints on recycling of potassium from
576 subducted ocean crust. Science, 272: 1972-1930.

577 Schmidt, M.W. and Poli, S. (1998) Experimentally based water budgets for dehydrating
578 slabs and consequences for arc magma generation. Earth and Planetary Science
579 Letters, 163: 361-379.

580 Schmidt, M.W. and Poli, S. (2014) Devolatilization during subduction. In R.L. Rudnick,
581 Ed., Treatise on Geochemistry: The Crust, 2nd ed., 3, p. 669-701. Elsevier,
582 Amsterdam.

583 Svensen, H., Bebout, G.E., Kronz, A., Li, L., Planke, S., Chevallier, L., and Jamtveit,
584 B. (2008) Nitrogen geochemistry as a tracer of fluid flow in a hydrothermal vent
585 complex in the Karoo Basin, South Africa. Geochimica et Cosmochimica Acta,
586 72: 4929-4947.

587 Tateyama, H., Shimda, S., and Sudo, T. (1977) Estimation of K-O distance and
588 tetrahedral rotation angle of K-micas from far-infrared absorption spectral data.
589 American Mineralogist, 62: 534-539.

590 Thompson, E.C., Campbell, A.J., and Liu, Z. (2016) In-situ infrared spectroscopic

591 studies of hydroxyl in amphiboles at high pressure. American Mineralogist, 101:
592 706-712.

593 Tokiwai, K. and Nakashima, S. (2010) Integral molar absorptivities of OH in muscovite
594 at 20 to 650 °C by in-situ high-temperature IR microspectroscopy. American
595 Mineralogist, 95: 1052-1059.

596 Vedder, W. (1965) Ammonium in muscovite. Geochimica et Cosmochimica Acta, 29:
597 221-228.

598 Vennari, C.E., O'Bannon, E.F., and Williams, Q. (2016) The ammonium ion in a silicate
599 under compression: infrared spectroscopy and powder X-ray diffraction of
600 $NH_4AlSi_3O_8$-buddingtonite to 30 GPa. Physics and Chemistry of Minerals, DOI
601 10.1007/s00269-016-0844-3.

602 Watenphul, A., Wunder, B., and Heinrich, W. (2009) High-pressure ammonium-bearing
603 silicates: implications for nitrogen and hydrogen storage in the Earth's mantle.
604 American Mineralogist, 94: 283-292.

605 Watenphul, A., Wunder, B., Wirth, R., and Heinrich, W. (2010) Ammonium-bearing
606 clinopyroxene: A potential nitrogen reservoir in the Earth's mantle. Chemical
607 Geology, 270: 240–248.

608 Weeks, T.J., Angell, C.L., and Bolton, A.P. (1975) The thermochemical properties of
609 ammonium exchanged erionite. Journal of Catalysis, 38: 461-468.

610 Whelan, J.K., Solomon, P.R., Desphande, G.V., and Carangelo, R.M. (1988)
611 Thermogravimetfic Fourier transform infrared spectroscopy (TG-FTIR) of
612 petroleum source rocks-initial results. Energy & Fuels, 2: 65-73.

613 Williams, L.B., Wilcoxon, B.R., Ferrell, R.E., and Sassen, R. (1992) Diagenesis of
614 ammonium during hydrocarbon maturation and migration, Wilcox Group,
615 Louisiana, USA. Applied Geochemistry, 7: 123-134.

616 Williams, Q., Knittle, E., Scott, H.P., and Liu, Z.X. (2012) The high--pressure behavior
617 of micas: Vibrational spectra of muscovite, biotite, and phlogopite to 30 GPa.

618 American Mineralogist, 97: 241-252.

619 Wunder, B., Berryman, E., Plessen, B., Rhede, D., Koch-Müller, M., and Heinrich, W.
620 (2015) Synthetic and natural ammonium-bearying tourmaline. American
621 Mineralgist, 100: 250-256.

622 Xu, H., Zhao, Y., Hickmott, D.D., Lane, N.J., Vogel, S.C., Zhang, J., and Daemen, L.L.
623 (2013): High-temperature neutron diffraction study of deuterated brucite. Physics
624 and Chemistry of Minerals, 40: 799-810.

625 Yang, Y., Xia, Q.K., Feng, M., and Zhang, P.P. (2010) Temperature dependence of IR
626 absorption of OH species in clinopyroxene. American Mineralogist, 95: 1439-
627 1443.

628 Yang, Y., Xia, Q.K., Feng, M., and Liu, S.C. (2012) OH in nature orthopyroxene: an in
629 situ FTIR investigation at varying temperatures. Physics and Chemistry of
630 Minerals, 39: 413-418.

631 Yang, Y., Xia, Q.K., and Zhang, P.P. (2015) Evolutions of OH groups in diopside and
632 feldspars with temperature. European Journal of Mineralogy, 27: 185-192.

633 Yokochi, R., Marty, B., Chazot, G., and Burnard, P. (2009) Nitrogen in peridotite
634 xenoliths: Lithophile behavior and magmatic isotope fractionation. Geochimica et
635 Cosmochimica Acta, 73: 4843-4861.

636 Zhang, M., Salje, E.K.H., Carpenter, M.A., Wang, J.Y., Groat, L.A., Lager, G.A., Wang,
637 L., Beran, A., and Bismayer, U. (2007) Temperature dependence of IR absorption
638 of hydrous/hydroxyl species in minerals and synthetic materials. American
639 Mineralogist, 92: 1502-1517.

640 Zhang, M., Redfern, S.T., Salje, E.K.H., Carpenter, M.A., and Hayward, C.L. (2010)
641 Thermal behavior of vibrational phonons and hydroxyls of muscovite in
642 dehydroxylation: In situ high-temperature infrared spectroscopic investigations.
643 American Mineralogist, 95: 1444-1457.

644 Table 1 Assignments of the observed IR and Raman bands in phengite at ambient

conditions

ν (cm^{-1})	Assignment
104	K-O stretching
192	M2-OH stretch. + Od xz-trans.
270	Ob, OH y-trans. + Oc, e z-trans. + K y-trans.
706	O out-of-plane Trans.+M-O Str.
1430	NH_4 bending band
2818	overtone antisymmetric bending
3036	combination of NH_4 symmetric and antisymmetric bending
3291	N-H stretching
3610	O-H stretching
4500	combination (O-H stretching and H-O-Si(Al) bending)

Note: The bands are assigned referring to Holtz et al. (1993), McKeown et al. (1999), Mookherjee and Redfern (2002), Busigny et al. (2003b), Zhang et al. (2010) and Williams et al. (2012), Mookherjee et al. (2012a and 2012b).

Figure captions:

Figure 1 The illustration of ammonium in the phengite structure. The crystal structure of phengite of 3T polytype is from Ivaldi et al. (2001).

Figure 2 (a) FTIR spectra of phengite (0.112 mm thickness) at room temperature; (b) A detailed view of the deconvolved ammonium bands. The marked bands originate from vibrations of ammonium and OH. The spectra are vertically offset for clarity.

Figure 3 *In situ* FTIR spectra of phengite (0.125 mm thickness) at low temperatures. Arrows indicates peak splitting at low temperatures. The dotted line is to guide the eye. The spectra are vertically offset for clarity.

Figure 4 *In situ* FTIR spectra of phengite (0.098 mm thickness) at high temperatures: (a) heating in air; (b) heating in Ar. The blue dotted lines are to show the new OH band appearing with increasing temperature, and the black dotted lines are to show the evolutions ammonium bands with temperature. The spectra are vertically offset for clarity.

Figure 5 Frequencies of (a) N-H stretching band and (b) bending band in phengite as a function of temperature. The error bars represent standard deviations which are obtained by performing

multiple fits on the spectra.

Figure 6 Time evolution of *in situ* IR spectra of phengite isothermally annealed at (a) 500 °C (using the grain with 0.084 mm thickness) and (b) 700 °C (using the grain with 0.115 mm thickness) in air. The spectra are vertically offset for clarity.

Figure 7 Room-temperature spectra recorded before and after the isothermal annealing for 30 min at (a) 750 °C (using the grain with 0.03 mm thickness) and (b) 800 ℃(using the grain with 0.01 mm thickness) in Ar. The spectra are vertically offset for clarity.

Figure 8 *In situ* Raman spectra of phengite (0.119 mm thickness) at high temperatures. The spectra are vertically offset for clarity.

Figure 9 Frequency shifts of lattice modes with temperature: (a) the 104 cm^{-1} band; (b) the 192 cm^{-1} band; (c) the 270 cm^{-1} band, and (d) 706 cm^{-1} band. The error bars represent standard deviations which are obtained by performing multiple fits on the spectra.

Figure 10 Schematic illustration of the mechanism of ammonium loss during the heating process.

This is a preprint, the final version is subject to change, of the American Mineralogist (MSA)
Cite as Authors (Year) Title. American Mineralogist, in press.
(DOI will not work until issue is live.) DOI: http://dx.doi.org/10.2138/am-2017-6094

Figure 1

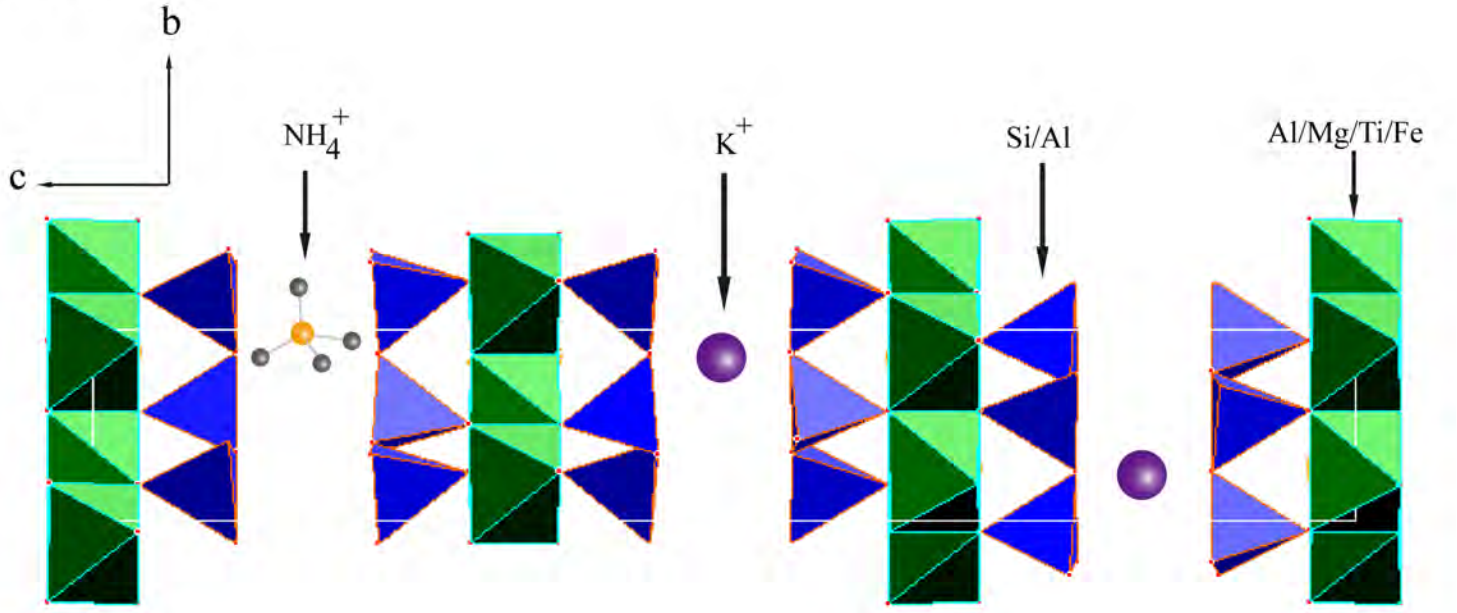

This is a preprint, the final version is subject to change, of the American Mineralogist (MSA)
Cite as Authors (Year) Title. American Mineralogist, in press.
(DOI will not work until issue is live.) DOI: http://dx.doi.org/10.2138/am-2017-6094

Figure 2

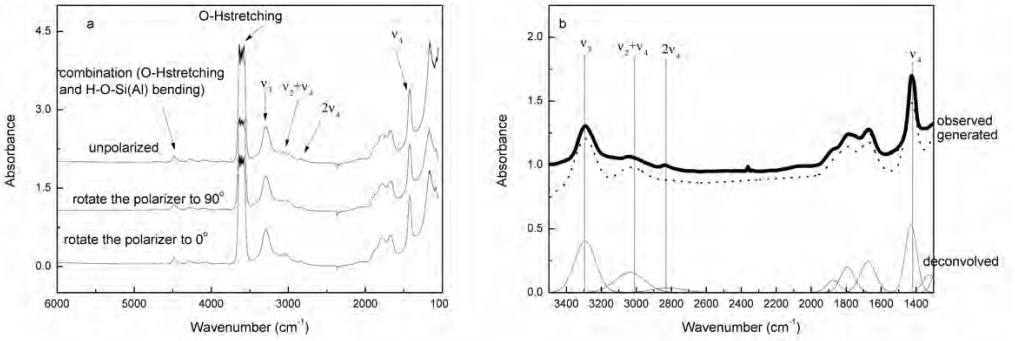

This is a preprint, the final version is subject to change, of the American Mineralogist (MSA)
Cite as Authors (Year) Title. American Mineralogist, in press.
(DOI will not work until issue is live.) DOI: http://dx.doi.org/10.2138/am-2017-6094

Figure 3

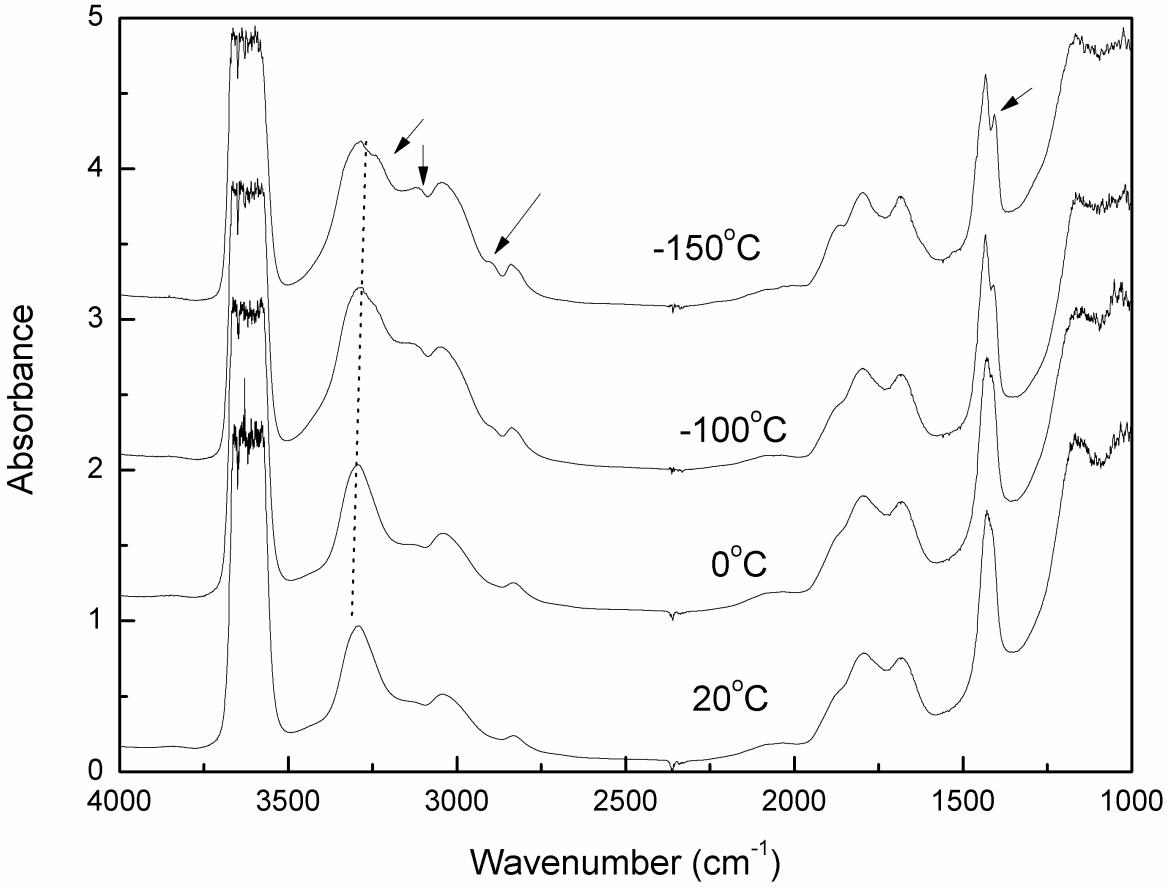

This is a preprint, the final version is subject to change, of the American Mineralogist (MSA)
Cite as Authors (Year) Title. American Mineralogist, in press.
(DOI will not work until issue is live.) DOI: http://dx.doi.org/10.2138/am-2017-6094

Figure 4

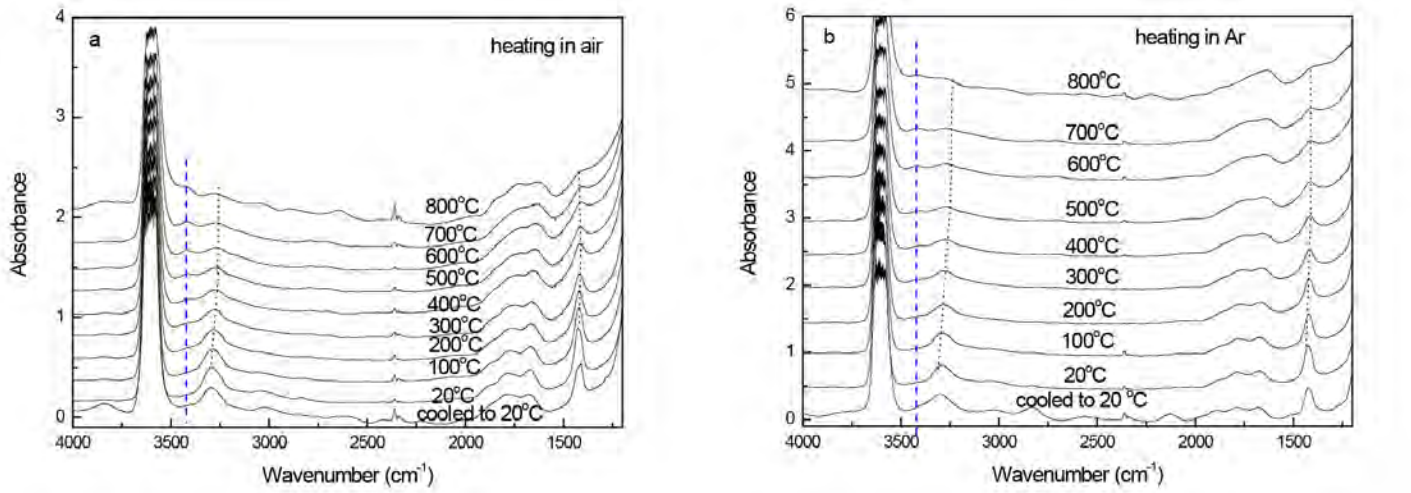

This is a preprint, the final version is subject to change, of the American Mineralogist (MSA)
Cite as Authors (Year) Title. American Mineralogist, in press.
(DOI will not work until issue is live.) DOI: http://dx.doi.org/10.2138/am-2017-6094

Figure 5

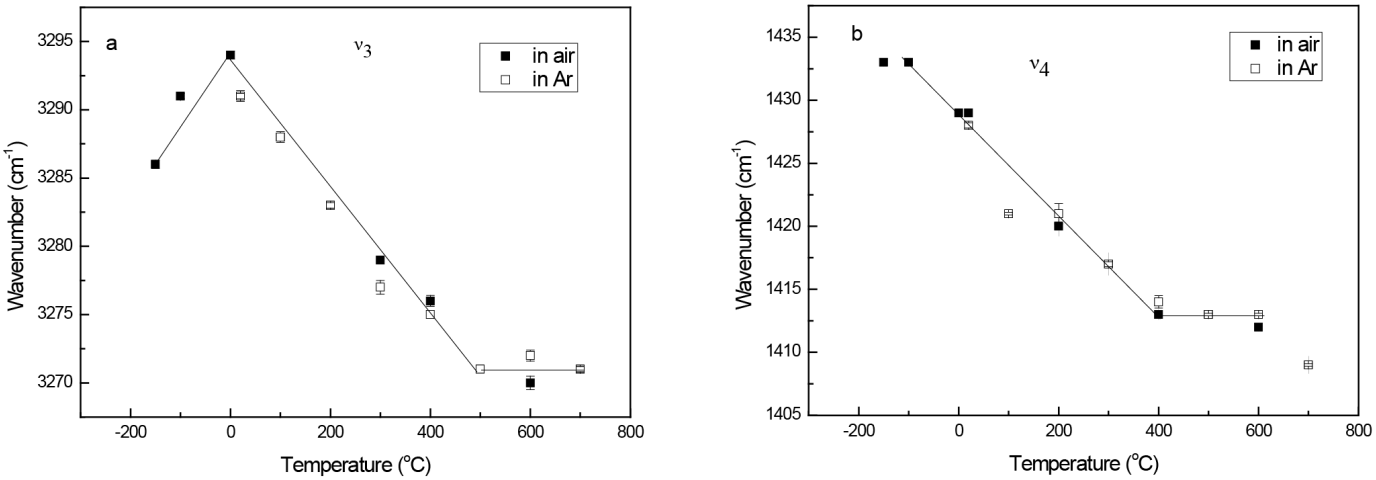

This is a preprint, the final version is subject to change, of the American Mineralogist (MSA)
Cite as Authors (Year) Title. American Mineralogist, in press.
(DOI will not work until issue is live.) DOI: http://dx.doi.org/10.2138/am-2017-6094

Figure 6

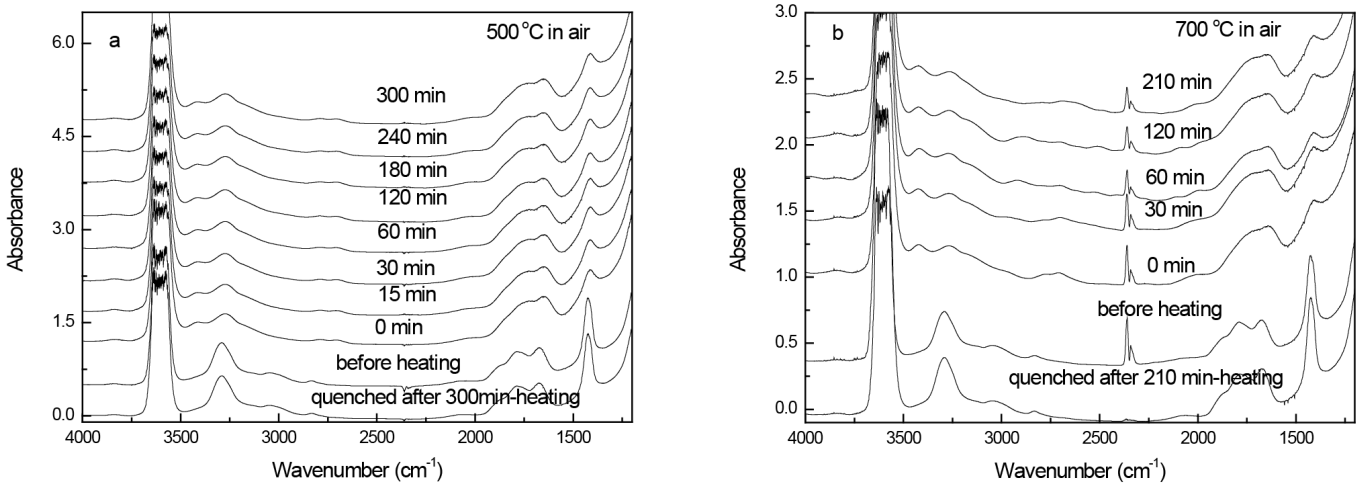

This is a preprint, the final version is subject to change, of the American Mineralogist (MSA)
Cite as Authors (Year) Title. American Mineralogist, in press.
(DOI will not work until issue is live.) DOI: http://dx.doi.org/10.2138/am-2017-6094

Figure 7

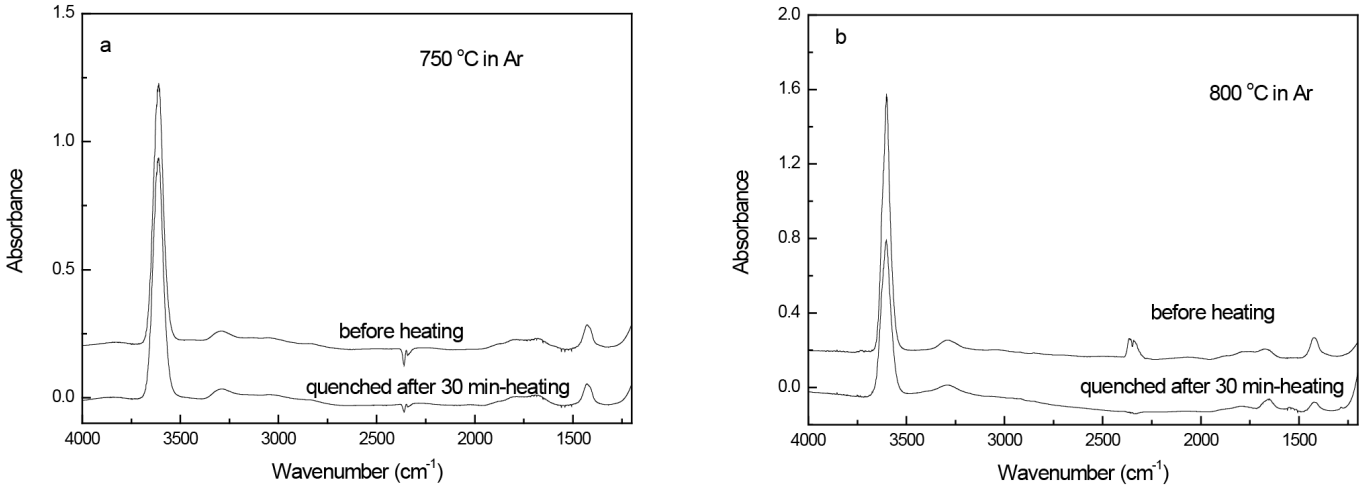

This is a preprint, the final version is subject to change, of the American Mineralogist (MSA)
Cite as Authors (Year) Title. American Mineralogist, in press.
(DOI will not work until issue is live.) DOI: http://dx.doi.org/10.2138/am-2017-6094

Figure 8

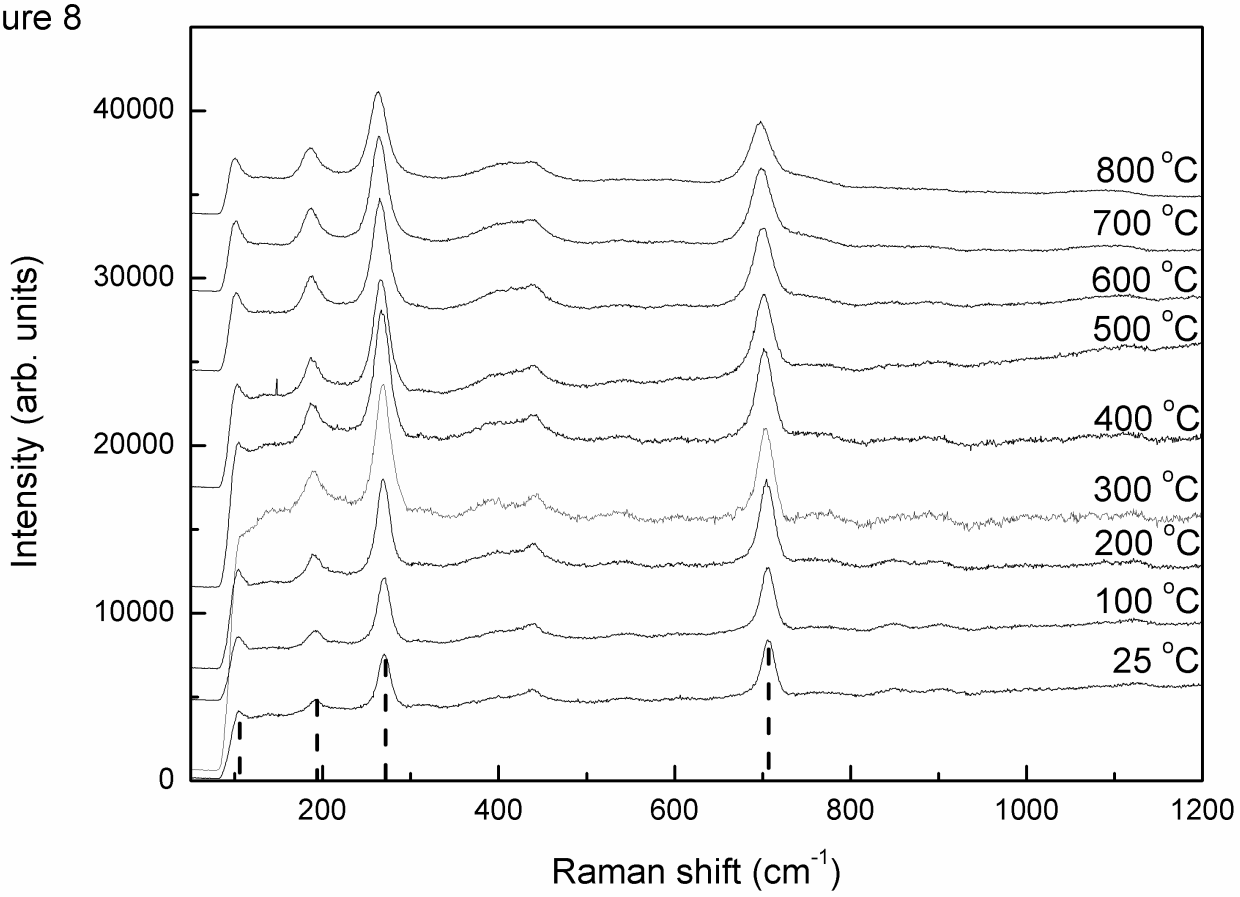

This is a preprint, the final version is subject to change, of the American Mineralogist (MSA)
Cite as Authors (Year) Title. American Mineralogist, in press.
(DOI will not work until issue is live.) DOI: http://dx.doi.org/10.2138/am-2017-6094

Figure 9

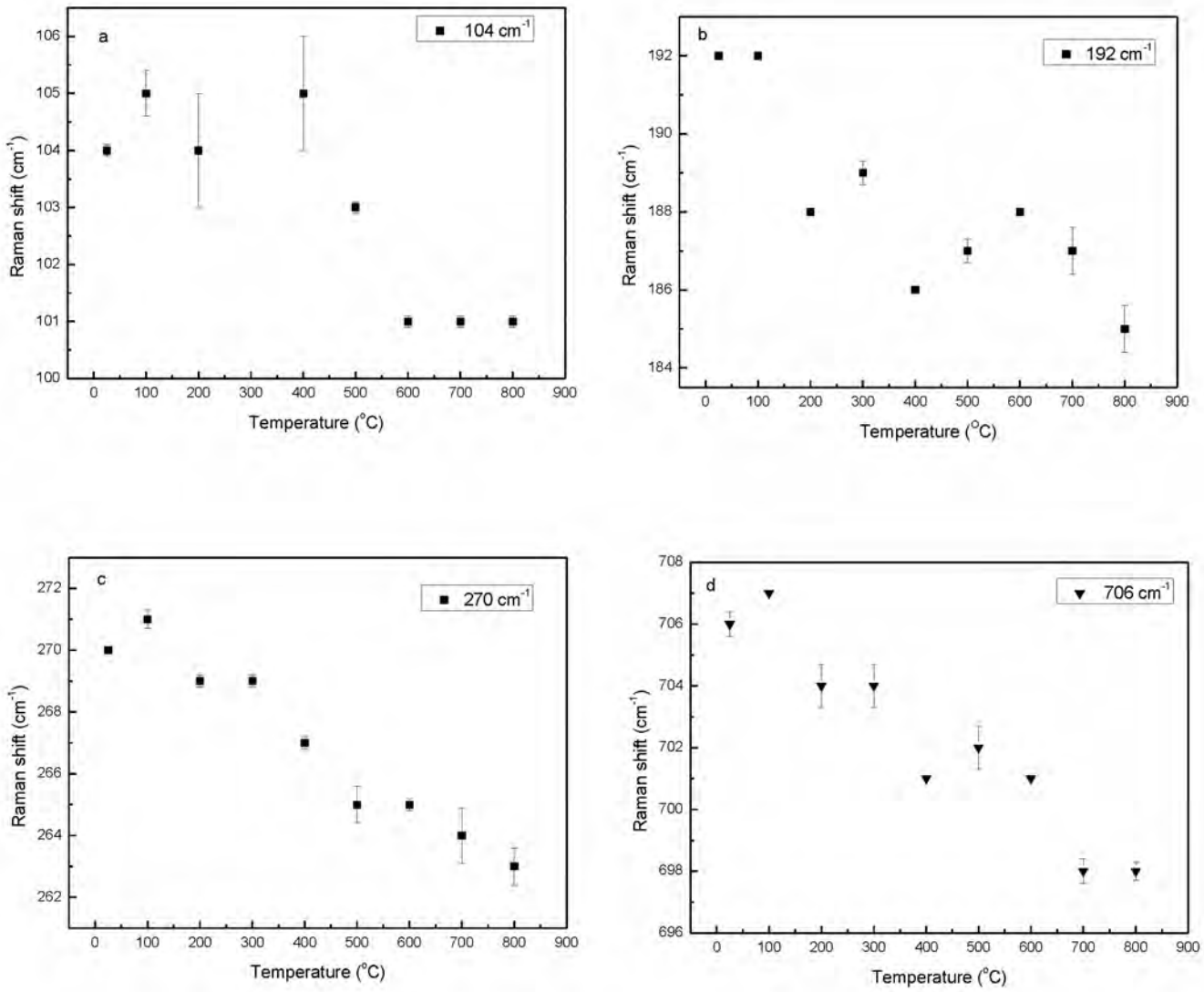

This is a preprint, the final version is subject to change, of the American Mineralogist (MSA)
Cite as Authors (Year) Title. American Mineralogist, in press.
(DOI will not work until issue is live.) DOI: http://dx.doi.org/10.2138/am-2017-6094

Figure 10